

[Weak] Gravitational Lensing

Martin Kilbinger

CEA Saclay, Irfu/SAP - AIM; IAP

Euclid Summer School, Narbonne
August 22 – 27, 2016

`martin.kilbinger@cea.fr`

`www.cosmostat.org/kilbinger`

`twitter.png`
`@energie_sombre`

Overview

Day 1: Principles of gravitational lensing

- Brief history of gravitational lensing
- Light deflection in an inhomogeneous Universe
- Convergence, shear, and ellipticity
- Projected power spectrum
- Real-space shear correlations

Day 2: Measurement of weak lensing

- Galaxy shape measurement
- PSF correction
- Photometric redshifts
- Estimating shear statistics

Day 3: Surveys and cosmology

- Cosmological modelling
- Results from past and ongoing surveys (CFHTlenS, KiDS, DES)
- Euclid

Day 3+: Extra stuff

Books, Reviews and Lecture Notes

- Bartelmann & Schneider 2001, review **Weak gravitational lensing**, Phys. Rep., 340, 297 arXiv:9912508
- Kochanek, Schneider & Wambsganss 2004, book (Saas Fee) **Gravitational lensing: Strong, weak & micro**, The third part (weak lensing) is available here: <http://www.astro.uni-bonn.de/~peter/SaaSFee.html>)
- Kilbinger 2015, review **Cosmology from cosmic shear observations** Reports on Progress in Physics, 78, 086901, arXiv:1411.0155
- Henk Hoekstra 2013, lecture notes (Varenna) arXiv:1312.5981
- Sarah Bridle 2014, lecture videos (Saas Fee) <http://saasfee2014.epfl.ch/page-110036-en.html>
- Alan Heavens, 2015, lecture notes (Rio de Janeiro) www.on.br/cce/2015/br/arq/Heavens_Lecture_4.pdf

Science with gravitational lensing

Outstanding results

Dark matter is not in form of massive compact objects (MACHOs).

Detection of Earth-mass exoplanets.

Structure of QSO inner emission regions.

Dark matter profiles in outskirts of galaxies.

Galaxy clusters are dominated by dark matter.

Constraints on dark energy and modified gravity.

Most important properties of gravitational lensing

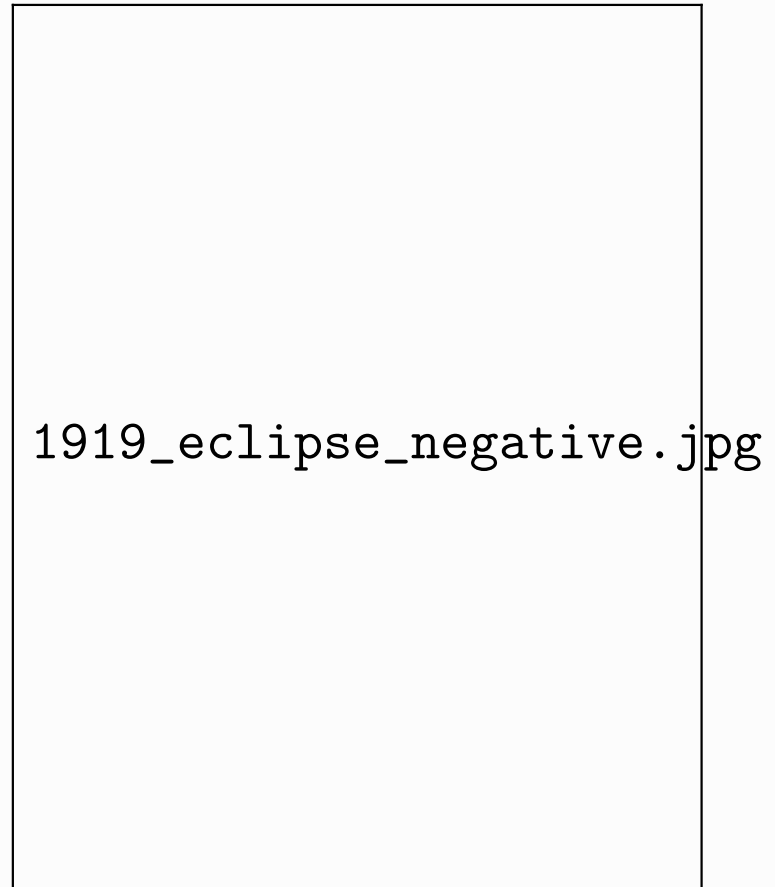
Lensing probes **total** matter, baryonic + dark.

Independent of dynamical state of matter.

Independent of nature of matter.

Brief history of gravitational lensing

- Before Einstein: Masses deflect photons, treated as point masses.
- 1915 Einstein's GR predicted deflection of stars by sun, deflection larger by 2 compared to classical value. Confirmed 1919 by Eddington and others during solar eclipse.



Photograph taken by Eddington of solar corona, and stars marked with bars.

Lensing on cosmological scales

zwicky.png

Abell-2151_LRGBha

- 1937 Zwicky posits galaxy clusters as lenses.
- 1979 Walsh et al. detect first double image of a lenses quasar.

Fritz Zwicky; Abell 2151 (Hercules galaxy cluster) ©Tony Hallas/APoD.

walsh_0957+561_spectra.jpg

(Walsh et al. 1979)

- 1987 Soucail et al. strongly distorted “arcs” of background galaxies behind galaxy cluster, using CCDs.

soucail_arc.pdf

soucail_arc_text.pdf

- Tyson et al. (1990), tangential alignment around clusters.

tyson_cluster_color.pdf

tyson_cluster_bw.pdf

Abell 1689

Cluster outskirts: Weak gravitational lensing.

- 2000 **cosmic shear**: weak lensing in blind fields, by 4 groups (Edinburgh, Hawai'i, Paris, Bell Labs/US).

Some 10,000 galaxies on few square degree on the sky area.

vW00+K13_xi_pm.pdf

Shear (ellipticity)
correlation of galaxies as
fct. of angular separation
(Van Waerbeke
et al. 2000, Kilbinger
et al. 2013).

- By 2016: Many dedicated surveys: DLS, CFHTLenS, DES, KiDS, HSC. Competitive constraints on cosmology.

Factor 100 increase: Millions of galaxies over 100s of degree area. Many other improvements: Multi-band observations, photometric redshifts, image and N -body simulations.

- By 2025: LSST, WFIRST-AFTA, Euclid data will be available.
Another factor of 100 increase:
Hundred millions of galaxies, tens of thousands of degree area (most of the extragalactic sky).

Euclid_survey.pdf

LSST-45-degree-full.jpg

Wfirst_MCR.jpg

Euclid_telescope.pdf

Types of lensing

`lensing_types_table_1.pdf`

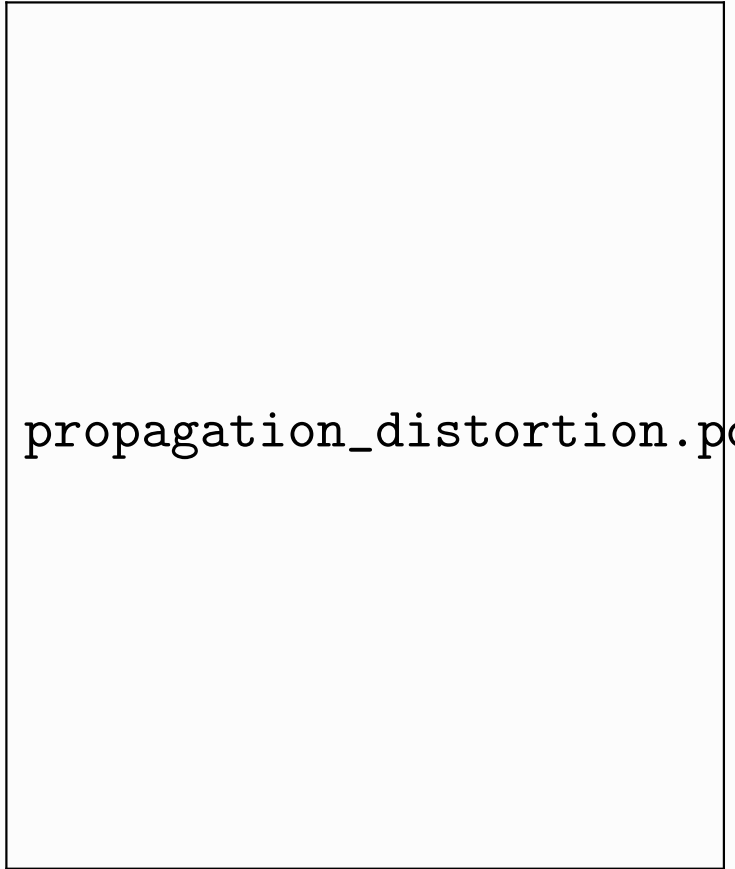
Types of lensing

`lensing_types_table_2.pdf`

Cosmic shear, or weak cosmological lensing

Light of distant galaxies is deflected while travelling through inhomogeneous Universe. Information about mass distributions is imprinted on observed galaxy images.

- Continuous deflection: sensitive to projected 2D mass distribution.
- Differential deflection: magnification, distortions of images.
- Small distortions, few percent change of images: need statistical measurement.
- Coherent distortions: measure correlations, scales few Mpc ... few 100 Mpc.



propagation_distortion.pdf

Deflection angle

Perturbed Minkowski metric, weak-field ($\phi \ll c^2$)

$$ds^2 = (1 + 2\phi/c^2) c^2 dt^2 - (1 - 2\phi/c^2) dl^2$$

One way to derive deflection angle: Fermat's principle:

Light travel time $t = \frac{1}{c} \int_{\text{path}} (1 - 2\phi/c^2) dl$

deflection-grad_sa.pdf

is stationary, $\delta t = 0$. (Analogous to geometrical optics, potential as medium with refract. index $n = 1 - 2\phi/c^2$.)
Integrate Euler-Lagrange equations along the light path to get

deflection angle $\hat{\alpha} = -\frac{2}{c^2} \int_S \nabla_{\perp} \phi dl$

Special case: point mass

Deflection angle for a point mass M is

$$\hat{\alpha} = \frac{4GM}{c^2} \frac{\xi}{\xi} = \frac{2R_S}{\xi} \frac{\xi}{\xi}$$

(R_S is the Schwarzschild radius.)

This is twice the value one would get in a classical, Newtonian calculation.

deflection_point_mass_scheme.pdf

einstein_ring_and_quasar.pdf

Exercise: Derive the deflection angle for a point mass. I

In the weak-field approximation, we can write the potential as

$$\phi = -\frac{GM}{R} = -\frac{c^2 R_S}{2 R},$$

where G is Newton's constant, M the mass of the object, R the distance, and R_S the Schwarzschild radius. The distance R can be written as $R^2 = x^2 + y^2 + z^2$.

(Here z is not redshift, but radial (comoving) distance.)

We use the so-called Born approximation (from quantum mechanic scattering theory) to integrate along the unperturbed light ray, which is a straight line parallel to the z -axis with a constant $x^2 + y^2 = \xi^2$. The impact parameter ξ is the distance of the light ray to the point mass.

The deflection angle is then

$$\hat{\alpha} = -\frac{2}{c^2} \int_{-\infty}^{\infty} \nabla_{\perp} \phi dz.$$

Exercise: Derive the deflection angle for a point mass. II

The perpendicular gradient of the potential is

$$\nabla_{\perp} \phi = \frac{c^2 R_S}{2|R|^3} \begin{pmatrix} x \\ y \end{pmatrix} = \frac{c^2 R_S}{2} \frac{\xi}{(\xi^2 + z^2)^{3/2}} \begin{pmatrix} \cos \varphi \\ \sin \varphi \end{pmatrix}.$$

The primitive for $(\xi^2 + z^2)^{-3/2}$ is $z\xi^{-2}(\xi^2 + z^2)^{-1/2}$. We use the symmetry of the integrand to integrate between 0 and ∞ , and get for the absolute value of the deflection angle

$$\hat{\alpha} = 2R_S \left[\frac{z}{\xi(\xi^2 + z^2)^{1/2}} \right]_0^{\infty} = \frac{2R_S}{\xi} = \frac{4GM}{c^2 \xi}.$$

Generalisation I: mass distribution

Distribution of point masses $M_i(\boldsymbol{\xi}_i, z)$: total deflection angle is linear vectorial sum over individual deflections

$$\hat{\alpha}(\boldsymbol{\xi}) = \sum_i \hat{\alpha}(\boldsymbol{\xi} - \boldsymbol{\xi}_i) = \frac{4G}{c^2} \sum_i M(\boldsymbol{\xi}_i, z) \frac{\boldsymbol{\xi} - \boldsymbol{\xi}_i}{|\boldsymbol{\xi} - \boldsymbol{\xi}_i|}$$

With transition to continuous density

$$M_i(\boldsymbol{\xi}_i, z) \rightarrow \int d^2\xi' \int dz' \rho(\boldsymbol{\xi}', z')$$

and introduction of the 2D

$$\text{surface mass density } \Sigma(\boldsymbol{\xi}') = \int dz' \rho(\boldsymbol{\xi}', z')$$

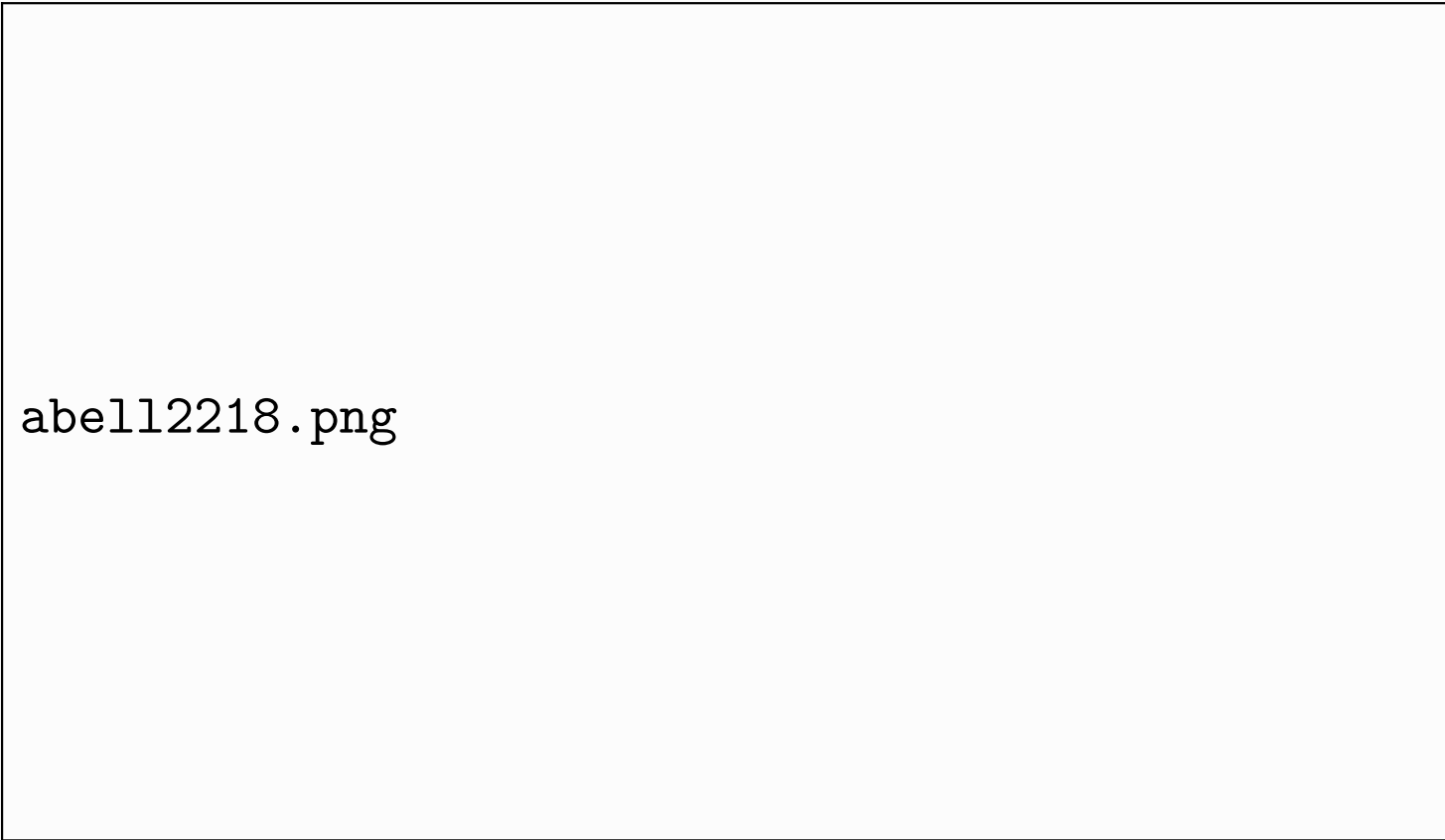
we get

$$\hat{\alpha}(\boldsymbol{\xi}) \int d^2\xi' \Sigma(\boldsymbol{\xi}') \frac{\boldsymbol{\xi} - \boldsymbol{\xi}_i}{|\boldsymbol{\xi} - \boldsymbol{\xi}_i|}$$

Thin-lens approximation

Generalisation II: Extended source I

Extended source: different light rays impact lens at different positions ξ , their deflection angle $\alpha(\xi)$ will be different: **differential deflection** \rightarrow distortion, magnification of source image!



abell12218.png

Propagation of light bundles I

Calculate deflection angle difference between different light bundles:



deflection-lss.pdf

In homogeneous flat Universe, transverse distance \boldsymbol{x}_0 between two light rays as fct. of comoving distance χ

$$\boldsymbol{x}_0(\chi) = \chi\boldsymbol{\theta}.$$

This is modified by inhomogeneous matter = deflectors as follows.

Propagation of light bundles II

From deflector at comoving distance χ' , infinitesimal deflection angle

$$d\hat{\alpha} = -\frac{2}{c^2} \nabla_{\perp} \phi(\mathbf{x}, \chi') d\chi'$$

This results in a change of transverse distance $d\mathbf{x}$ from vantage point of deflector (at χ')

$$d\mathbf{x} = (\chi - \chi') d\hat{\alpha}$$

Total deflection: integrate over all deflectors along χ' . This would yield the difference between a perturbed and an unperturbed light ray. To account for perturbation of second light ray, subtract gradient of potential $\phi^{(0)}$ along second light ray.

$$\mathbf{x}(\chi) = \chi\boldsymbol{\theta} - \frac{2}{c^2} \int_0^{\chi} d\chi' (\chi - \chi') \left[\nabla_{\perp} \phi(\mathbf{x}(\chi'), \chi') - \nabla_{\perp} \phi^{(0)}(\chi') \right].$$

Transform distances into angles seen from the observer: divide by χ . \mathbf{x}/χ is the angle $\boldsymbol{\beta}$ under which the unlensed source is seen. The integral/ χ is the

Propagation of light bundles III

geometric difference between unlensed (β) and apparent, lensed (θ) is the **deflection angle**

$$\alpha = \frac{2}{c^2} \int_0^x d\chi' \frac{\chi - \chi'}{\chi} \left[\nabla_{\perp} \Phi(\mathbf{x}(\chi'), \chi') - \nabla_{\perp} \Phi^{(0)}(\chi') \right].$$

This results in the **lens equation**

$$\beta = \theta - \alpha.$$

This is a mapping from lens coordinates θ to source coordinates β . (Q: why not the other way round?)

Linearized lensing quantities I

To 0th order: approximate light path \mathbf{x} , on which potential gradient is evaluated in integral with unperturbed line $\chi\boldsymbol{\theta}$ (**Born approximation**):

$$\boldsymbol{\beta}(\boldsymbol{\theta}) = \boldsymbol{\theta} - \frac{2}{c^2} \int_0^{\chi} d\chi' \frac{\chi - \chi'}{\chi} \left[\nabla_{\perp} \Phi(\chi'\boldsymbol{\theta}, \chi') - \nabla_{\perp} \Phi^{(0)}(\chi') \right].$$

This neglects coupling between structures at different distances (*lens-lens coupling*): Distortion at some distance adds to undistorted image, neglecting distortion effect on already distorted image by all matter up to that distance.

Numerical simulations show that Born is accurate to sub-percent on most scales. This is pretty cool. Differences between perturbed and unperturbed light ray can be a few Mpc!

Next, drop the second term (does not depend on distance $\mathbf{x} = \chi\boldsymbol{\theta}$, so gradient vanishes).

Linearized lensing quantities II

Now, we can move the gradient out of integral. That means, deflection angle is a gradient of a potential, the 2D **lensing potential** ψ . Writing derivatives with respect to angle $\boldsymbol{\theta}$, we get

$$\boldsymbol{\beta}(\boldsymbol{\theta}, \chi) = \boldsymbol{\theta} - \nabla_{\boldsymbol{\theta}}\psi(\boldsymbol{\theta}, \chi)$$

with

$$\psi(\boldsymbol{\theta}, \chi) = \frac{2}{c^2} \int_0^\chi d\chi' \frac{\chi - \chi'}{\chi\chi'} \phi(\chi'\boldsymbol{\theta}, \chi').$$

[Note: Above equations are valid for flat Universe. For general (curved) models, some comoving distances are replaced by comoving angular distances.]

Linearized lensing quantities III

Linearizing lens equation

We talked about differential deflection before. To first order, this involves the derivative of the deflection angle.

Or the lens mapping:

$$\frac{\partial \beta_i}{\partial \theta_j} \equiv A_{ij} = \delta_{ij} - \partial_i \partial_j \psi.$$

Jacobi (symmetric) matrix

$$A = \begin{pmatrix} 1 - \kappa - \gamma_1 & -\gamma_2 \\ -\gamma_2 & 1 - \kappa + \gamma_1 \end{pmatrix}.$$

- **convergence** κ : isotropic magnification
- **shear** γ : anisotropic stretching

Convergence and shear are second derivatives of the 2D lensing potential.



kappagamma.pdf

Convergence and shear I

The effect of κ and γ follows from Liouville's theorem: Surface brightness is conserved (no photon gets lost).

Therefore the surface brightness I at the lensed position $\boldsymbol{\theta}$ is equal to the unlensed, **source** surface brightness I^s at the source position $\boldsymbol{\beta}$.

$$I(\boldsymbol{\theta}) = I^s(\boldsymbol{\beta}(\boldsymbol{\theta})) \approx I^s(\boldsymbol{\beta}(\boldsymbol{\theta}_0) + \mathcal{A}(\boldsymbol{\theta} - \boldsymbol{\theta}_0))$$

Example: circular isophotes

Effect can easily be seen for circular source isophotes, e.g. $\theta_1 = R \cos t, \theta_2 = R \sin t$ (thus $\theta_1^2 + \theta_2^2 = R^2$).

Convergence

Applying the Jacobi matrix with zero shear (and setting $\boldsymbol{\beta}(\boldsymbol{\theta}_0) = 0$), we find $\beta_1^2 + \beta_2^2 = R^2(1 - \kappa)^2$. The radius R of these isophotes gets transformed at source position to $R(1 - \kappa)$.

Convergence and shear II

Shear

To see an example for the shear stretching, set $\gamma_2 = 0$. We find

$(\beta_1, \beta_2) = R([1 - \kappa - \gamma_1] \cos t, [1 - \kappa + \gamma_1] \sin t)$ and thus

$(\beta_1/[1 - \kappa - \gamma_1])^2 + (\beta_2/[1 - \kappa + \gamma_1])^2 = R^2$, which is an ellipse with half axes $R/[1 - \kappa - \gamma_1]$ and $R/[1 - \kappa + \gamma_1]$.

So we see that **shear** transforms a circular image into an elliptical one.

Define complex shear

$$\gamma = \gamma_1 + i\gamma_2 = |\gamma|e^{2i\varphi};$$

The relation between convergence, shear, and the axis ratio of elliptical isophotes is then

$$|\gamma| = |1 - \kappa| \frac{1 - b/a}{1 + b/a}$$

ellipsedef.pdf

Convergence and shear III

Further consequence of lensing: **magnification**.

Liouville (surface brightness is conserved) + area changes ($d\beta^2 \neq d\theta^2$ in general) \rightarrow flux changes.

$$\text{magnification } \mu = \det A^{-1} = [(1 - \kappa)^2 - \gamma^2]^{-1}.$$

Summary: Convergence and shear linearly encompass information about projected mass distribution (lensing potential ψ). They quantify how lensed images are magnified, enlarged, and stretched. These are the main observables in (weak) lensing.

Effects of lensing, $\partial^i \psi / \partial x^i$

di_dpsi_effects_sun.pdf

Basic equation of weak lensing

Weak lensing regime

$$\kappa \ll 1, |\gamma| \ll 1.$$

The observed ellipticity of a galaxy is the sum of the intrinsic ellipticity and the shear:

$$\boxed{\varepsilon \approx \varepsilon^s + \gamma}$$

Random intrinsic orientation of galaxies

$$\langle \varepsilon^s \rangle = 0 \quad \longrightarrow \quad \boxed{\langle \varepsilon \rangle = \gamma}$$

The observed ellipticity is an unbiased estimator of the shear. Very noisy though! $\sigma_\varepsilon = \langle |\varepsilon^s|^2 \rangle^{1/2} \approx 0.4 \gg \gamma \sim 0.03$. Increase S/N and beat down noise by averaging over large number of galaxies.

Question: Why is the equivalent estimation of the convergence and/or magnification more difficult?

Ellipticity and local shear

mellfig02.pdf

[from Y. Mellier]

Galaxy ellipticities are an estimator of the local shear.

Some weak-lensing galaxy surveys

Survey	Date	Area [deg ²]	n_{gal} [arcmin ⁻²]
CFHTLenS	2003-2007	170	14
DLS	2001-2006	25	20
COSMOS	2005	1.6	80
SDSS	2000-2012	11,000	2
KiDS	2011-	1,500	7-8
HSC	2015-	1,500	~ 20
DES	2012-2018	5,000	5-6
LSST	2021-	15,000	~ 20
Euclid	2021-2026	15,000	~ 25
WFIRST-AFTA	2024-	2,500	?

Convergence and cosmic density contrast

Back to the lensing potential

- Since $\kappa = \frac{1}{2}\Delta\psi$:

$$\kappa(\boldsymbol{\theta}, \chi) = \frac{1}{c^2} \int_0^\chi d\chi' \frac{(\chi - \chi')\chi'}{\chi} \Delta\Phi(\chi'\boldsymbol{\theta}, \chi')$$

- Terms $\Delta_{\chi'\chi'}\Phi$ average out when integrating along line of sight, can be added to yield 3D Laplacian (error $\mathcal{O}(\Phi) \sim 10^{-5}$).
- Poisson equation

$$\Delta\Phi = \frac{3H_0^2\Omega_m}{2a} \delta \quad \left(\delta = \frac{\rho - \bar{\rho}}{\rho} \right)$$

$$\rightarrow \kappa(\boldsymbol{\theta}, \chi) = \frac{3}{2}\Omega_m \left(\frac{H_0}{c} \right)^2 \int_0^\chi d\chi' \frac{(\chi - \chi')\chi'}{\chi a(\chi')} \delta(\chi'\boldsymbol{\theta}, \chi').$$

Amplitude of the cosmic shear signal

Order-of magnitude estimate

$$\kappa(\boldsymbol{\theta}, \chi) = \frac{3}{2} \Omega_m \left(\frac{H_0}{c} \right)^2 \int_0^\chi d\chi' \frac{(\chi - \chi')\chi'}{\chi a(\chi')} \delta(\chi' \boldsymbol{\theta}, \chi').$$

for simple case: single lens at redshift $z_L = 0.4$ with comoving size $R/a(z_L)$, source at $z_S = 0.8$.

$$\kappa \approx \frac{3}{2} \Omega_m \left(\frac{H_0}{c} \right)^2 \frac{D_{LS} D_L}{D_S} \frac{R}{a^2(z_L)} \frac{\delta\rho}{\rho}$$

Add signal from $N \approx D_S/R$ crossings, calculate rms:

$$\begin{aligned} \langle \kappa^2 \rangle^{1/2} &\approx \frac{3}{2} \Omega_m \frac{D_{LS} D_L}{R_H^2} \sqrt{\frac{R}{D_S}} a^{-1.5}(z_L) \left\langle \left(\frac{\delta\rho}{\rho} \right)^2 \right\rangle^{1/2} \\ &\approx \frac{3}{2} 0.3 \times 0.1 \times 0.1 \times 2 \times 1 \approx 0.01 \end{aligned}$$

We are indeed in the weak-lensing regime.

Convergence with source redshift distribution

So far, we looked at the convergence for one **single** source redshift (distance χ). Now, we calculate κ for a realistic survey with a redshift **distribution** of source galaxies. We integrate over the pdf $p(\chi)d\chi = p(z)dz$, to get

$$\kappa(\boldsymbol{\theta}) = \int_0^{\chi_{\text{lim}}} d\chi p(\chi) \kappa(\boldsymbol{\theta}, \chi) = \int_0^{\chi_{\text{lim}}} d\chi G(\chi) \chi \delta(\chi\boldsymbol{\theta}, \chi)$$

with **lens efficiency**

$$G(\chi) = \frac{3}{2} \left(\frac{H_0}{c} \right)^2 \frac{\Omega_m}{a(\chi)} \int_{\chi}^{\chi_{\text{lim}}} d\chi' p(\chi') \frac{\chi' - \chi}{\chi'}.$$

The convergence is a projection of the matter-density contrast, weighted by the source galaxy distribution and angular distances.

Parametrization of redshift distribution, e.g.

$$p(z) \propto \left(\frac{z}{z_0}\right)^\alpha \exp\left[-\left(\frac{z}{z_0}\right)^\beta\right]$$

prob_default1.pdf

G_default1.pdf

$$\alpha = 2, \beta = 1.5, z_0 = 1$$

(dashed line: all sources at redshift 1)

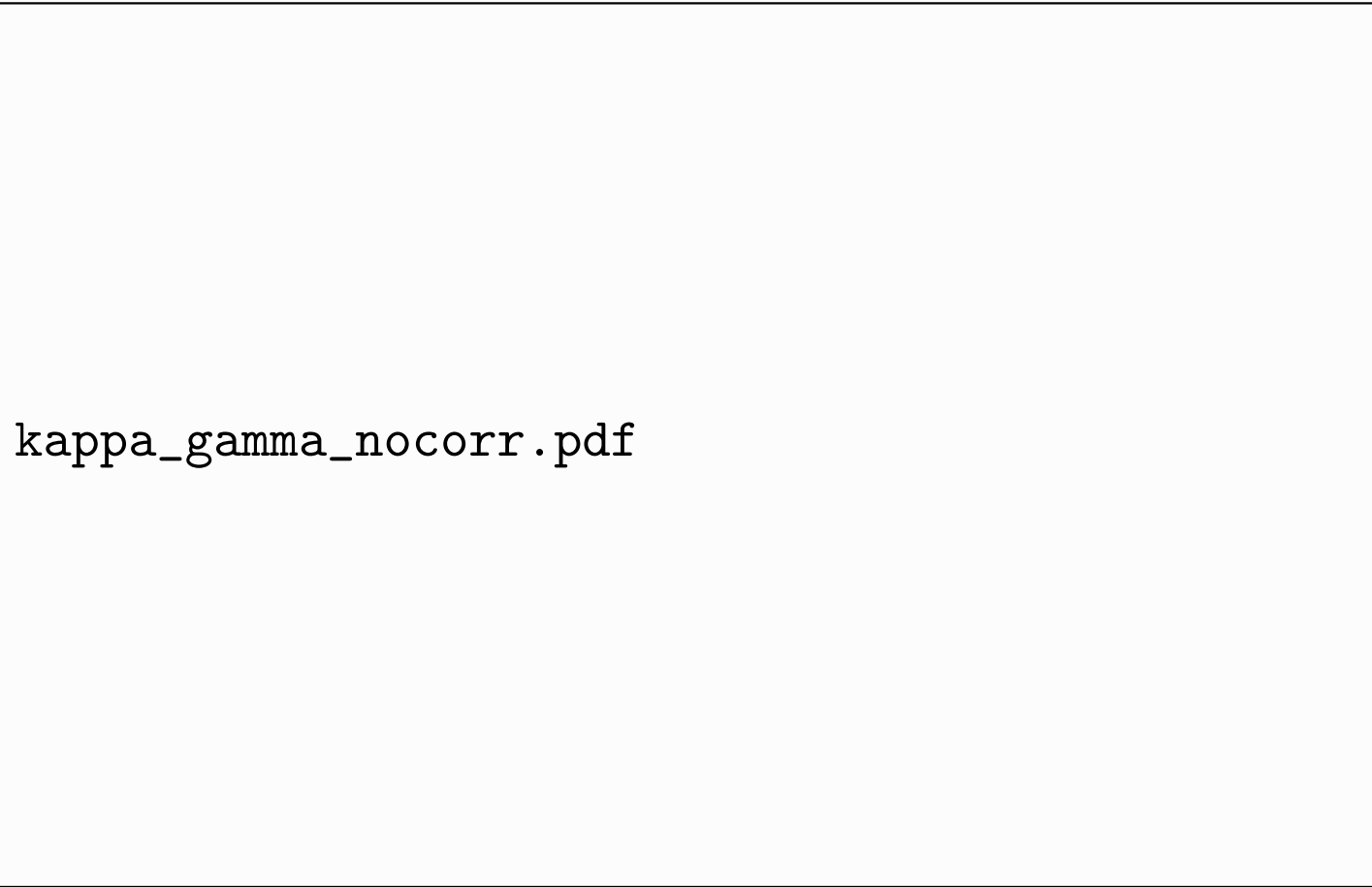
Max. lensing signal from halfway distance between us and lensing galaxies.

More on the relation between κ and γ

Convergence and shear are second derivatives of lensing potential \rightarrow they are related.

One can derive κ from γ (except constant *mass sheet* κ_0).

E.g. get projected **mass reconstruction** of clusters from ellipticity observations.



kappa_gamma_nocorr.pdf

More on the relation between κ and γ

Convergence and shear are second derivatives of lensing potential \rightarrow they are related.

Fluctuations (variance σ^2) in κ and γ are the same!

E.g. get variance/**power spectrum** of projected δ from ellipticity correlations.

kappa_gamma_wcorr.pdf

The convergence power spectrum

- Variance of convergence $\langle \kappa(\boldsymbol{\vartheta} + \boldsymbol{\theta})\kappa(\boldsymbol{\vartheta}) \rangle = \langle \kappa\kappa \rangle(\boldsymbol{\theta})$ depends on variance of the density contrast $\langle \delta\delta \rangle$
- In Fourier space:

$$\begin{aligned}\langle \hat{\kappa}(\boldsymbol{\ell})\hat{\kappa}^*(\boldsymbol{\ell}') \rangle &= (2\pi)^2 \delta_{\text{D}}(\boldsymbol{\ell} - \boldsymbol{\ell}') P_{\kappa}(\ell) \\ \langle \hat{\delta}(\mathbf{k})\hat{\delta}^*(\mathbf{k}') \rangle &= (2\pi)^3 \delta_{\text{D}}(\mathbf{k} - \mathbf{k}') P_{\delta}(k)\end{aligned}$$

- **Limber's equation**

$$P_{\kappa}(\ell) = \int d\chi G^2(\chi) P_{\delta} \left(k = \frac{\ell}{\chi} \right)$$

using small-angle approximation, $P_{\delta}(k) \approx P_{\delta}(k_{\perp})$, contribution only from Fourier modes \perp to line of sight. Also assumes that power spectrum varies slowly.

Dependence on cosmology

pkappa_dep_chi.pdf

Example

A simple toy model: single lens plane at redshift z_0 , $P_\delta(k) \propto \sigma_8^2 k^n$, CDM, no Λ , linear growth:

$$\langle \kappa^2(\theta) \rangle^{1/2} = \langle \gamma^2(\theta) \rangle^{1/2} \approx 0.01 \sigma_8 \Omega_m^{0.8} \left(\frac{\theta}{1\text{deg}} \right)^{-(n+2)/2} z_0^{0.75}$$

This simple example illustrates three important facts about measuring cosmology from weak lensing:

1. The signal is very small (\sim percent)
2. Parameters are degenerate
3. The signal depends on source galaxy redshift

Lensing ‘tomography’ (2 1/2 D lensing)

- Bin galaxies in redshift.
- Lensing efficiency different for different bins (even though the probed redshift range is overlapping): measure z -depending expansion and growth history.
- Necessary for dark energy, modified gravity.

$$P_{\kappa}(\ell) = \int_0^{\chi_{\text{lim}}} d\chi G^2(\chi) P_{\delta} \left(k = \frac{\ell}{\chi} \right) \rightarrow$$

$$P_{\kappa}^{ij}(\ell) = \int_0^{\chi_{\text{lim}}} d\chi G_i(\chi) G_j(\chi) P_{\delta} \left(k = \frac{\ell}{\chi} \right)$$

$$G_i(\chi) = \frac{3}{2} \left(\frac{H_0}{c} \right)^2 \frac{\Omega_m}{a(\chi)} \int_{\chi}^{\chi_{\text{lim}}} d\chi' p_i(\chi') \frac{\chi' - \chi}{\chi'}.$$

shear_tomography.pdf

pkappa.pdf

Convergence power spectrum for two different redshift bins
($0 = [0.5; 0.7]$, $1 = [0.9; 1.1]$).

Unlike CMB C_ℓ 's, features in matter power spectrum are washed out by projection and non-linear evolution.

anddP_kappa-fig3_review.pdf

Correlations of two shears I

We have established **lensing power spectrum** $P_\kappa = P_\gamma$ (power spectrum of projected δ) as interesting quantity for cosmology.

kappa_gamma_extract.pdf

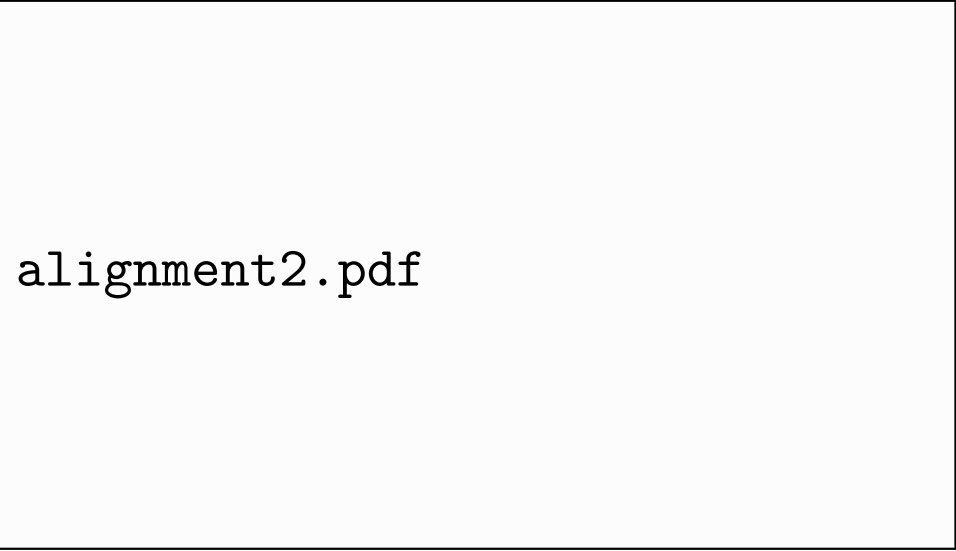
Provides theory model prediction correlation of κ or γ in Fourier space. However we measure shear (ellipticity) in real space.

Two options to make connection:

1. Fourier-transform data. Square to get power spectrum.
2. Calculate correlations in real space. Inverse-Fourier transform theory P_κ .

Correlations of two shears II

Correlation of the shear at two points yields four quantities



alignment2.pdf

Parity conservation $\longrightarrow \langle \gamma_t \gamma_x \rangle = \langle \gamma_x \gamma_t \rangle = 0$

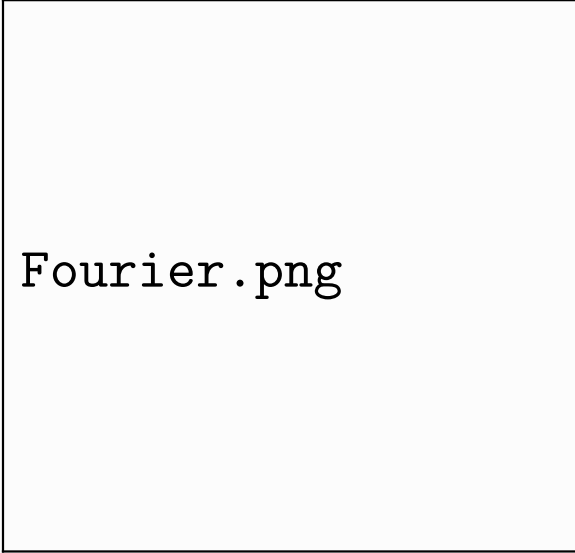
The two components of the shear **two-point correlation function** (2PCF) are defined as

$$\xi_+(\vartheta) = \langle \gamma_t \gamma_t \rangle(\vartheta) + \langle \gamma_x \gamma_x \rangle(\vartheta)$$

$$\xi_-(\vartheta) = \langle \gamma_t \gamma_t \rangle(\vartheta) - \langle \gamma_x \gamma_x \rangle(\vartheta)$$

Correlations of two shears III

The 2PCF is the 2D Fourier transform of the lensing power spectrum.



Fourier.png

Isotropy \rightarrow 1D integrals, *Hankel transform*.

$$\xi_+(\theta) = \frac{1}{2\pi} \int_0^\infty dl \, l J_0(l\theta) P_\kappa(l)$$
$$\xi_-(\theta) = \frac{1}{2\pi} \int_0^\infty dl \, l J_4(l\theta) P_\kappa(l),$$

E- and B-modes I

Shear patterns

We have seen tangential pattern in the shear field due to mass over-densities. Under-dense regions cause a similar pattern, but with opposite sign for γ . That results in radial pattern.

Under idealistic conditions, these are the only possible patterns for a shear field, the *E*-mode. A so-called *B*-mode is not generated.



Emode.pdf



Bmode.pdf

E- and B-modes II

Origins of a B-mode

Measuring a non-zero B-mode in observations is usually seen as indicator of residual systematics in the data processing (e.g. PSF correction, astrometry).

Other origins of a B-mode are small, of %-level:

- Higher-order terms beyond Born approximation (propagation along perturbed light ray, non-linear lens-lens coupling), and other (e.g. some ellipticity estimators)
- Lens galaxy selection biases (size, magnitude biases), and galaxy clustering
- Intrinsic alignment (although magnitude not well-known!)
- Varying seeing and other observational effects

E- and B-modes III

Measuring E- and B-modes

Separating data into E- and B-mode is not trivial.

To directly obtain κ^E and κ^B from γ , there is leakage between modes due to the finite observed field (border and mask artefacts).

One can quantify the shear pattern, e.g. with respect to reference centre points, but the tangential shear γ_t is not defined at the center.

Solution: **filter** the shear map. (= convolve with a filter function Q). This also has the advantage that the spin-2 quantity shear is transformed into a scalar.

This is equivalent to filtering κ with a function U that is related to Q .